Ultra-Compact and Low-Loss Polarization Rotator Based on Asymmetric Hybrid Plasmonic Waveguide

Linfei Gao, Yijie Huo, James S. Harris, and Zhiping Zhou

***Abstract*— We propose a novel hybrid plasmonic polarization rotator based on mode interference. Operating at the telecommunication wavelength of 1.55 μm, the rotation length is very short (3.2 μm), while the polarization conversion efficiency is as high as 99.5%. The total device insertion loss is only 1.38 dB, much smaller than the common level of plasmonic devices. It also has potential to realize integrated waveplates for various polarization states.**

***Index Terms*— Integrated optical devices, polarization rotators, plasmonics, silicon photonics.**

I. Introduction

POLARIZATION rotators (PRs) are of great importance in photonic integrated circuits (PICs) [1], especially for SOI platforms which suffer from high polarization sensitivity induced by high index contrast. Several different approaches have been proposed to realize on-chip PRs, such as mode evolution [2], [3] mode interference[4]–[6] and asymmetrical directional coupling [7]. In terms of single waveguide based devices, mode evolution schemes usually require rather long lengths (>100 μm) to obtain adiabatic mode conversion, while mode interference schemes can be much shorter. However, to realize on chip mode interference schemes, the symmetry of standard waveguides must be broken to obtain the required mode optical axes rotation. Unfortunately, the limited candidate materials exhibiting unicity on the SOI platform provide little freedom for design. Most existing designs are realized by geometrically modifying Si waveguides (e.g. slanted waveguides [4] and narrow trenches [5]) and have either complicated fabrication processes [4], or long device lengths (600 μm) [5]. Therefore, a new mechanism with both a simple structure and good performance is urgently needed.

Manuscript received June 30, 2013; revised August 20, 2013; accepted September 4, 2013. Date of publication September 11, 2013; date of current version October 4, 2013. This work was supported in part by the Major International Cooperation and Exchange Program of the National Natural Science Foundation of China under Grant 61120106012, in part by the National High Technology Research and Development Program of China under Grant 2011AA010302, and in part by the China Scholarship Council under Grant 201206010200.

L. Gao is with the State Key Laboratory of Advanced Optical Communication Systems and Networks, Peking University, Beijing 100871, China, and also with the Department of Electrical Engineering, Stanford University, Stanford, CA 94305 USA (e-mail: linfei@stanford.edu).

Y. Huo and J. S. Harris are with the Department of Electrical Engineering, Stanford University, Stanford, CA 94305 USA (e-mail: yjhuo@stanford.edu; jharris@stanford.edu).

Z. Zhou is with the State Key Laboratory of Advanced Optical Communication Systems and Networks, Peking University, Beijing 100871, China (e-mail: zjzhou@pku.edu.cn).

Color versions of one or more of the figures in this letter are available online at http://ieeexplore.ieee.org.

Digital Object Identifier 10.1109/LPT.2013.2281425

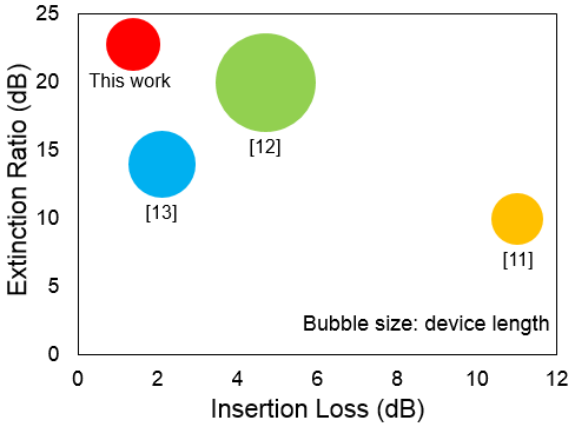

Fig. 1. Summary of extinction ratios, insertion losses, and device lengths of reported plasmonic polarization rotators.

Meanwhile, plasmonics is emerging and promising for compact polarization-selective devices due to its natural polarization sensitivity and unique ability for driving photonic devices into nano-scale dimensions [8]–[10]. Recent pioneering research has demonstrated plasmonic polarization rotators [11]–[14]. However, most of these rotators use the mode evolution principle. Their performances are summarized in Fig. 1. Ref. [11] uses a plasmonic waveguide with no/ very thin (~10 nm) spacer between metal and Si. The device size is quite small (3μm) due to a strong plasmonic effect, but at the cost of large material losses. Ref. [12] and [13] use the same principle of mode evolution as Ref. [11], but their waveguides include a larger spacer (50~110 nm) between metal and Si to reduce loss effects from metal. However, the device length is relatively long (Ref. [12] 11μm and Ref. [13] 5 μm). In summary, although plasmonics helps shrink the device length to the order of several or tens of micrometers, it is still hard to obtain both good performance and small size simultaneously. The tradeoff comes from the physical limitation of the mode evolution principle: a long distance is required to obtain adiabatic mode conversion with low losses; yet, longer lengths would accumulate larger Ohmic losses from the metal. Therefore, our work aims at breaking this limitation by using a different operation principle with the plasmonic effect.

Recently, hybrid plasmonic waveguides (HPWs) have attracted increasing attention [15]–[20]. A HPW is usually composed of a metal cap, a thin low-index dielectric layer and a high-index dielectric layer. Modes in the HPW could be seen as a combination of surface plasmon modes at the metal/low index interface and traditional photonic modes in

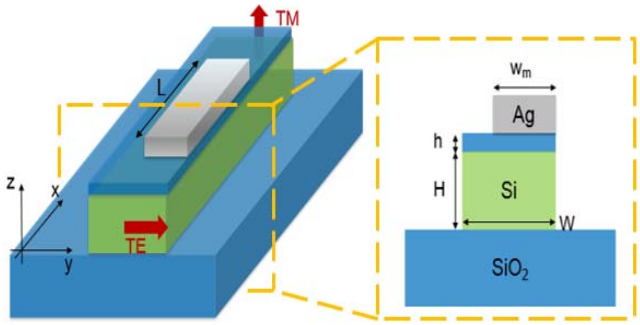

Fig. 2. Three-dimension schematic of the proposed device and the cross section of the polarization rotation section.

high-index waveguide. Therefore, they have outstanding properties of both low propagation losses and strong confinement. Furthermore, they could be fabricated using standard processes on SOI platforms and the consistency between experiment and modeling has been well proven [17], [19]. Based on this, some functional devices have been proposed using HPWs, such as polarization splitters [20].

In this letter, we propose an ultra-compact plasmonic polarization rotator based on a specifically designed asymmetric HPW. Instead of the mode evolution principle that is usually used in plasmonic PRs [11]–[13], our device is based on mode interference. To the best of our knowledge, this is the first time a mode interference-based polarization rotator has been solely realized by the plasmonic effect. Due to the metal induced asymmetry, the optical axis of two eigenmodes are rotated, and their propagation constants have a large difference, leading to an ultra-short half interference length (3.2 μm). It shows a high polarization conversion efficiency of 99.5%, while the insertion loss is only 1.38 dB, much smaller than the general level for plasmonic devices. The structure is quite simple to design and fabricate [17]. It also paves the way to achieve integrated waveplates, driving many important optical functions from free space onto a chip.

II. Structure and Principle

As shown in Fig. 2, the proposed device is built on an SOI substrate with a Si top layer of 250 nm height. It includes input and output sections formed by silicon wire waveguides. The rotation section between input and output sections is a HPW composed of a silver cap with thickness of 100 nm separated from the Si core by a thin SiO_2 gap. Different from common HPWs, here the metal only covers part of the Si core in our structure, *i.e.* $w_m < W$. Therefore, the structure's symmetry is broken and it could support two hybrid modes whose optical axes are rotated 45° with respect to the z axis, as shown in Fig. 3. The length of the rotation waveguide, L, equals to the half interference length $L_c = \pi/(\beta_1 - \beta_2)$, where β_1 and β_2 are the propagation constants of the two hybrid modes. If we consider a y-polarized input light, *i.e.* TE polarization, it will excite the two hybrid modes in the asymmetric HPW. Then the two modes beat with each other and accumulate a π-phase shift after travelling through the rotation section. Finally, TM polarization is obtained at the output waveguide. This structure also works for the TM input case.

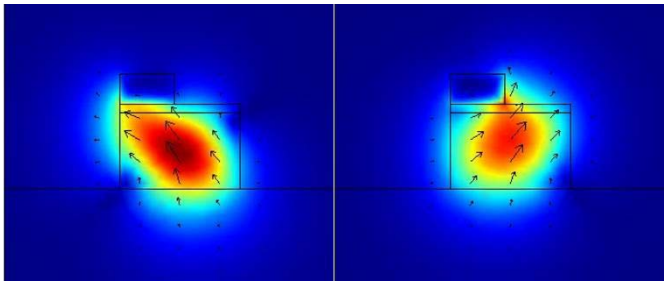

Fig. 3. Magnetic field profiles of two hybrid modes in the asymmetric HPW when $\theta = 45°$. Arrow: magnetic field direction. Here $W = 400$ nm, $h = 30$ nm, and $w_m = 182$ nm.

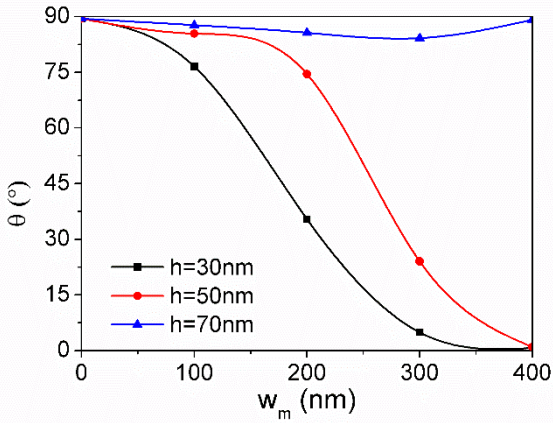

Fig. 4. Variation of optical axis rotation angle with respect to the metal width. Here W is fitted to be 400 nm.

A key figure of merit for a polarization rotator is the polarization conversion efficiency (PCE), which is defined as the output power ratio of the desired polarization to the sum of both polarizations, i.e. PCE = $P_{TM}/(P_{TE}+P_{TM})$. For mode interference schemes, PCE is directly related to the hybrid mode optical axis rotation angle [4]

$$\mathrm{PCE} = \sin^2(2\theta)\sin^2\left(\frac{\pi L}{2L_c}\right). \tag{1}$$

Here the rotation angle (θ) is defined as [4]

$$\tan(\theta) = R = \iint \frac{\varepsilon(y,z)E_y^2(y,z)dydz}{\varepsilon(y,z)E_Z^2(y,z)dydz}, \tag{2}$$

where ε(y,z) is the real part of permittivity distribution, Ey(y,z) and Ez(y,z) are the transverse and horizontal electrical components of an eigenmode, and R is the polarization rotation parameter. Accordingly, $\theta = 45°$ is required to realize 100% PCE.

Therefore, the analysis of optical axis rotation is very important to design the polarization rotator. Notably, it is the asymmetric metal that causes the optical axis rotation, so we calculate θ as a function of metal width, w_m, at different gap heights, h, while Si width, W, is set to be a fitted value of 400 nm. The calculation is carried out by the finite element method. The operating wavelength is 1.55 μm, and the corresponding indices of Si, SiO_2 and Ag are 3.455, 1.445 and 0.1453+11.3547i [21], respectively. According to Fig. 4, at $h = 30$ nm or 50 nm, θ experiences a decrease from 90° to 0° when increasing w_m from 0 to W. The desirable

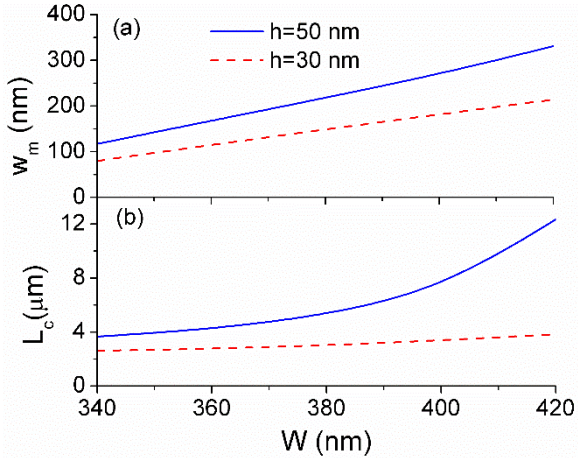

Fig. 5. (a) Metal width w_m and (b) half beating length L_c as a function of W at $\theta = 45°$.

45° can be obtained when choosing a proper value of w_m. However, an interesting phenomenon is that when h is larger, like 70 nm, θ is always around 90°. This is partially because for a larger h, the metal is farther away from the Si waveguide, thus its influence becomes too weak to rotate the optical axis. Therefore, h should not be too large as to allow the metal to become influential enough on the modes. However, the propagation loss is larger at smaller h [16]–[18]. Therefore, there is a trade-off between choices for an optimum value of h. More details of these trade-offs will be discussed below.

Additionally, θ at various values of W is further explored. We find that $\theta = 45°$ can be obtained over a large range of combinations of W, w_m and h, as demonstrated in Fig. 5(a). One sees that w_m decreases almost linearly as W decreases. This provides a guide on how to adjust parameters accordingly in the experiment after one layer has been fabricated. The corresponding half interference length as a function of W is shown in Fig. 5(b). Here w_m is set to the values on the curves in Fig. 5(a) for $\theta = 45°$. For $h = 50$ nm, L_c increases dramatically as W increases. In contrast with $h = 30$ nm, L_c remains relatively constant at quite a small value of ~ 3 μm. Based on this point it is beneficial to choose a smaller h in consideration of the compact size. On the other hand, as mentioned above, the propagation loss is larger at a smaller value of h, or a smaller value of W [16], [17]. The propagation losses of the two hybrid modes are calculated separately. For example, when $h = 30$ nm, and $W = 400$ nm, the propagation losses of the two eigen hybrid modes are 0.046 and 0.032 dB/μm, respectively. Therefore, the total loss after propagating through half the interference length of ~ 3 μm is very small. Since L_c does not vary much with W at $h = 30$ nm, we can realize both short length and low loss by choosing a larger W and a smaller h. Moreover, these parameters are all quite readily achieved in terms of today's fabrication technology.

III. Results and Discussion

In order to verify the design principles and demonstrate expected performance, three-dimensional finite difference time domain (3D-FDTD) simulations were carried out. Here we set

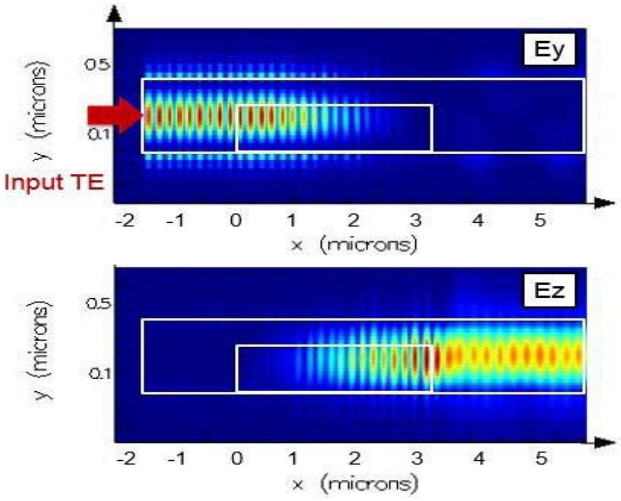

Fig. 6. Ey and Ez distribution in the device when TE light (Ey dominant) is input from the left port. Here $W = 400$ nm, $w_m = 180$ nm, $h = 30$ nm and $L = 3.2$ μm.

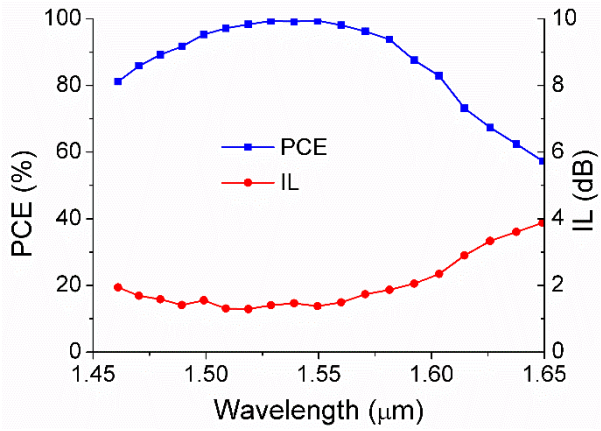

Fig. 7. Wavelength dependence of polarization conversion efficiency and insertion loss.

$h = 30$ nm and $W = 400$ nm. The optimized values of w_m and L by FDTD simulation are 180 nm and 3.2 μm respectively, which fit well with the results in Fig. 5. The simulated field distributions of Ey and Ez are shown in Fig. 6. One sees that when TE polarized light is launched, its dominant component Ey fades away in the rotation section. By contrast, Ez begins to appear in the rotation section and becomes dominant in the output section. Consequently, TE polarization is rotated to TM polarization. The PCE is 99.5% for a wavelength of 1.55 μm. The other two important parameters, extinction ratio (ER) and insertion loss (IL) are defined as

$$\begin{aligned} \mathrm{ER} &= 10\lg(P_{\mathrm{TM}}/P_{\mathrm{TE}}), \\ \mathrm{IL} &= -10\lg(P_{\mathrm{TM}}/P_{\mathrm{Input}}). \end{aligned} \tag{3}$$

The results for ER and IL are 22.4 dB and 1.38 dB, respectively. Here the insertion loss includes all the possible losses during the device operation, such as coupling loss between sections, scattering loss and propagation loss induced by the metal. It could be further reduced by using tapered structures.

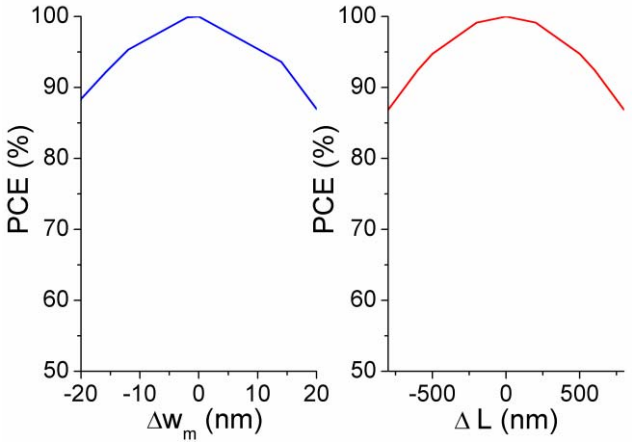

Fig. 8. Dependence of PCE on deviation of metal width w_m and metal length L.

The spectral responses of PCE and IL are plotted in Fig. 7. For a common requirement of PCE over 92% [7], the bandwidth is as large as 100 nm, while IL maintains a very low level, *i.e.* below 1.9 dB. Specifically, for the entire C band PCE is larger than 97% and ER is over 16 dB. The huge bandwidth makes the device available for many applications, including dense wavelength division multiplexing systems. In addition, the fabrication tolerance is analyzed. Fig. 8 shows PCE as a function of metal width and length variations. The tolerance of w_m is around 30 nm (-15 nm $< \Delta w_m <$ 15 nm) for PCE over 92%, which can be easily controlled by modern nano fabrication. Meanwhile, the performance is not sensitive to variations of L, whose tolerance is hundreds of nanometers.

IV. Conclusion

In summary, a mode-interference based polarization rotator can be realized in an asymmetric hybrid plasmonic waveguide. It is one of the shortest polarization rotators with a rotation length of only 3.2 μm. The polarization conversion efficiency is high (99.5%) while the total insertion loss is as low as 1.38 dB. The structure is easy to design and fabricate. It could be fully CMOS- compatible by using other metals such as Al, while the metal induced loss will not affect muchbecause of the ultra-short device length. This structure provides a new approach to the design of compact and low loss polarization-selective devices using the plasmonic effect. In addition, this scheme could also work as an integrated waveplate to realize a large range of functions in various applications.

References

[1] T. Barwicz, *et al.*, "Polarization-transparent microphotonic devices in the strong confinement limit," *Nature Photon.*, vol. 1, pp. 57–60, Dec. 2006.
[2] J. Zhang, M. Yu, G.-Q. Lo, and D.-L. Kwong, "Silicon-waveguide-based mode evolution polarization rotator," *IEEE J. Sel. Topics Quantum Electron.*, vol. 16, no. 1, pp. 53–60, Jan./Feb. 2010.
[3] L. Chen, C. Doerr, and Y.-K. Chen, "Compact polarization rotator on silicon for polarization-diversified circuits," *Opt. Lett.*, vol. 36, no. 4, pp. 469–471, Feb. 2011.
[4] H. Deng, D. O. Yevick, C. Brooks, and P. E. Jessop, "Design rules for slanted-angle polarization rotators," *J. Lightw. Technol.*, vol. 23, no. 1, pp. 432–445, Jan. 2005.
[5] K. Nakayama, Y. Shoji, and T. Mizumoto, "Single trench SiON waveguide TE-TM mode converter," *IEEE Photon. Technol. Lett.*, vol. 24, no. 15, pp. 1310–1312, Aug. 1, 2012.
[6] Z. Wang and D. Dai, "Ultrasmall Si-nanowire-based polarization rotator," *J. Opt. Soc. Amer. B, Opt. Phys.*, vol. 25, no. 5, pp. 747–753, May 2008.
[7] L. Liu, Y. Ding, K. Yvind, and J. M. Hvam, "Efficient and compact TE-TM polarization converter built on silicon-on-insulator platform with a simple fabrication process," *Opt. Lett.*, vol. 36, no. 7, pp. 1059–1061, Apr. 2011.
[8] W. L. Barnes, A. Dereux, and T. W. Ebbesen, "Surface plasmon subwavelength optics," *Nature*, vol. 424, pp. 824–830, Aug. 2003.
[9] E. Ozbay, "Plasmonics: Merging photonics and electronics at nanoscale dimensions," *Science*, vol. 311, no. 5758, pp. 189–193, Jan. 2006.
[10] D. K. Gramotnev and S. I. Bozhevolnyi, "Plasmonics beyond the diffraction limit," *Nature Photon.*, vol. 4, pp. 83–91, Jan. 2010.
[11] J. Zhang, S. Zhu, H. Zhang, S. Chen, G. O. Lo, and D. L. Kwong, "An ultra-compact surface plasmon polariton-effect-based polarization rotator," *IEEE Photon. Technol. Lett.*, vol. 23, no. 21, pp. 1606–1608, Nov. 1, 2011.
[12] M. Komatsu, K. Saitoh, and M. Koshiba, "Compact polarization rotator based on surface plasmon polariton with low insertion loss," *IEEE Photon. J.*, vol. 4, no. 3, pp. 707–714, Jun. 2012.
[13] J. N. Caspers, M. Z. Alam, and M. Mojahedi, "Compact hybrid plasmonic polarization rotator," *Opt. Lett.*, vol. 37, no. 22, pp. 4615–4617, Nov. 2012.
[14] H.-S. Kim, T.-K. Lee, G.-Y. Oh, B.-H. Lee, D.-G. Kim, and Y.-W. Choi, "Compact polarization rotator based on slotted optical waveguide with buffer layer using surface plasmon polariton," *Proc. SPIE*, vol. 8619, pp. 861923-1–861923-6, Mar. 2013.
[15] R. F. Oulton, V. J. Sorger, D. A. Genov, D. F. P. Pile, and X. Zhang, "A hybrid plasmonic waveguide for subwavelength confinement and long-range propagation," *Nature Photon.*, vol. 2, no. 8, pp. 496–500, Jul. 2008.
[16] D. Dai and S. He, "A silicon-based hybrid plasmonic waveguide with a metal cap for a nano-scale light confinement," *Opt. Express*, vol. 17, no. 19, pp. 16646–16653, Sep. 2009.
[17] M. Wu, Z. Han, and V. Van, "Conductor-gap-silicon plasmonic waveguides and passive components at subwavelength scale," *Opt. Express*, vol. 18, no. 11, pp. 11728–11736, May 2010.
[18] L. Gao, L. Tang, F. Hu, R. Guo, X. Wang, and Z. Zhou, "Active metal strip hybrid plasmonic waveguide with low critical material gain," *Opt. Express*, vol. 20, no. 10, pp. 11487–11495, May 2012.
[19] V. J. Sorger, *et al.*, "Experimental demonstration of low-loss optical waveguiding at deep sub-wavelength scales," *Nature Commun.*, vol. 2, no. 331, pp. 1–5, May 2011.
[20] L. Gao, F. Hu, X. Wang, L. Tang, and Z. Zhou, "Ultracompact and silicon-on-insulator-compatible polarization splitter based on asymmetric plasmonic–dielectric coupling," *Appl. Phys. B*, 2013, doi: 10.1007/s00340-013-5457-7.
[21] P. B. Johnson and R. W. Christie, "Optical constants of the noble metals," *Phys. Rev. B*, vol. 6, no. 12, pp. 4370–4379, Dec. 1972.